Article **Journal Electrical Engineering**
December 2023, Vol.7 No.19 1-14

Development of an electronic stethoscope implementing filters with OPAM for the observation of cardiac signals using a graphical interface with an AD8232 module

Desarrollo de un estetoscopio electrónico implementando filtros con OPAM para la observación de señales cardíacas utilizando una interfaz gráfica con un módulo AD8232

GONZÁLEZ-GALINDO, Edgar Alfredo†*, RÍOS-MENDOZA, Fernando Javier, CASTRO-PÉREZ, Joseph Kevin and DOMÍNGUEZ-ROMERO, Francisco Javier

Universidad Nacional Autónoma de México, Facultad de Estudios Superiore Aragón, Centro Tecnológic Aragón, Measurement and Instrumentation and Control Laboratory. Mexico.

ID 1st Author: *Edgar Alfredo, González-Galindo* / **ORC ID:** 0000-0003-4654-9595, **Researcher ID Thomson:** G-7927-2018, **CVU CONACYT ID:** 351785

ID 1st Co-author: *Fernando Javier Ríos-Mendoza* **/ ORC** ID 0009-0008-7125-0150, **Researcher ID Thomson:** HTS-9088-2023, **CVU CONACYT ID** 1039711

ID 2nd Co-author: *Joseph Kevin, Castro-Pérez* / ORC ID 0000-0001-6755-5260, **Researcher ID Thomson:** HJY-8903-2023, **CVU CONACYT ID** 1266037

ID 3rd Co-author: *Francisco Javier, Domínguez-Romero* / **ORC ID:** 0000-0003-0578-9322, **Researcher ID Thomson:** AFD-9764-2022, **CVU CONACYT ID:** 1037122

DOI: 10.35429/JEE.2023.19.7.1.14 Received July 10, 2023; Accepted December 30, 2023

Abstract

In this article, an investigation was developed in a clinic A low-cost electronic stethoscope has been developed, which utilizes fourth-order active filters and a TL081 operational amplifier preamplifier. It incorporates the AD8232 module for monitoring cardiac signals and features a graphical interface for visualizing these signals. A schematic circuit was designed for a second-order active filter with preamplifiers to compensate for signal attenuation, and electret microphones were used to replace the headphones. The device was implemented using an Arduino development board and a printed circuit board for connecting modules such as the AD8232, DS3231, and MicroSD. The system generates an audible signal through speakers, and the graphical interface facilitates the visualization of the electrical signal captured by the electrodes on the test subject. Data is recorded with date and time thanks to the DS3132 module and stored on the MicroSD module. The objective is to provide an affordable electronic stethoscope with a graphical interface that can be used in both medical clinics and homes during emergencies when access to a hospital electrocardiogram is not always possible. This low-cost solution provides an accessible and reliable tool for monitoring cardiac signals, improving healthcare in various clinical scenarios.

AD8232, DS3132, MicroSD

Resumen

Se ha desarrollado un estetoscopio electrónico de bajo costo que utiliza filtros activos de cuarto orden y un preamplificador con el amplificador operacional TL081. Incorpora el módulo AD8232 para monitoreo de señales cardíacas y cuenta con interfaz gráfica para visualizar dichas señales. Se diseñó un circuito esquemático para un filtro activo de segundo orden con preamplificadores para compensar la atenuación de la señal, y se reemplazaron los auriculares por micrófonos electret. El dispositivo se implementó con una tarjeta de desarrollo Arduino y un circuito impreso para conexión de módulos como AD8232, DS3231 y MicroSD. El sistema genera una señal audible a través de altavoces, y la interfaz gráfica facilita la visualización de la señal eléctrica capturada por los electrodos en el sujeto de prueba. Los datos se registran con fecha y hora gracias al módulo DS3132 y se almacenan en el módulo MicroSD. El objetivo es proporcionar un estetoscopio electrónico asequible con interfaz gráfica, válido tanto en consultorios médicos como en hogares durante emergencias, cuando no siempre es posible acceder a un electrocardiograma hospitalario. Esta solución de bajo costo brinda una herramienta accesible y confiable para el monitoreo de señales cardíacas, mejorando la atención médica en diversas situaciones clínicas.

AD8232, DS3132, MicroSD

Citation: GONZÁLEZ-GALINDO, Edgar Alfredo, RÍOS-MENDOZA, Fernando Javier, CASTRO-PÉREZ, Joseph Kevin and DOMÍNGUEZ-ROMERO, Francisco Javier. Development of an electronic stethoscope implementing filters with OPAM for the observation of cardiac signals using a graphical interface with an AD8232 module. Journal Electrical Engineering. 2023. 7-19:1-14.

* Correspondence to the author (E-mail: unam_alf@comunidad.unam.mx)
† Researcher contributing as first author.

Introduction

Today, cardiac problems can arise from two categories of causes. On the one hand, there are drugs, such as catecholamines, phosphodiesterase inhibitors, digitalis, beta-adrenergic stimulants and atropine. On the other hand, there are pathological processes, including cardiomyopathies, fibrosis, hyperkalaemia and ischaemia. In addition, it has been observed that severe acute respiratory syndrome, caused by SARS-CoV2, can have cardiac sequelae in the post-pandemic phase. This is because the severe cardiorespiratory distress caused by the virus can be further complicated if the individual has previous comorbidities. The World Health Organisation (WHO) provided data indicating that cardiovascular disease (CVD) is the leading cause of death worldwide.

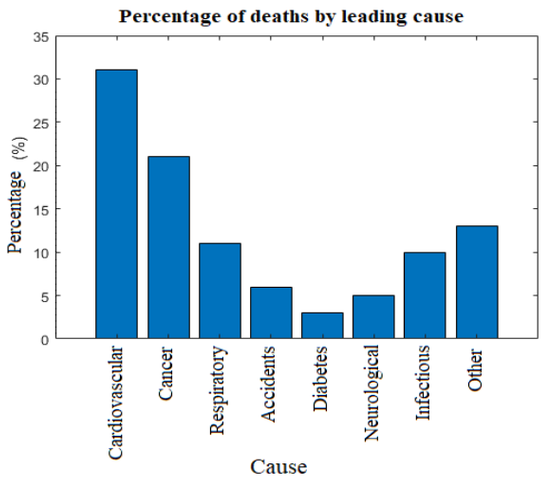

Graphic 1 Deaths from major diseases worldwide

In 2017, an estimated 17.9 million people died from CVD, accounting for 31% of all deaths worldwide. For the latest data, I would recommend searching for heart disease statistics on the WHO website or other reliable sources of public health information. When citing these sources, be sure to follow the correct citation format depending on the style you are using (WHO,2023). During 2021, heart disease emerged as the leading cause of death in Mexico, culminating in a total of 226,703 deaths. This number marked an increase of 8,000 deaths compared to the previous year. Among heart diseases, atrial fibrillation is the most prevalent arrhythmia worldwide, affecting approximately 40 million people. In Mexico, it is estimated that more than half a million people suffer from this condition (Bibiano, 2023).

The stethoscope was invented by French physician René Laennec in 1816. Laennec invented the stethoscope because he felt uncomfortable placing his ear on his patients' chests to listen to internal sounds, a common practice at the time (Roguin, 2006).

The stethoscope has gone through several modifications since René Laennec first invented it. However, one of the most notable changes was made by the Irish physician Arthur Leared in 1851. It was Leared who proposed the binaural design (two earpieces), which is the model that prevails to this day (Langfort, 1999). The stethoscope is a fundamental medical instrument used for auscultation, or listening to the internal sounds of the human body. In the 20th century, stethoscope technology continued to improve, with the introduction of electronic stethoscopes that could amplify body sounds for better diagnosis. Today, the stethoscope remains an essential tool in medical practice, used to listen to the sounds of the heart, lungs and abdomen (Bassetti, 2019). Therefore digital stethoscopes emerged as a superior option, offering sound amplification, more consistent frequency response and active noise cancellation. In addition, they have become a valuable tool for teaching auscultation due to their ease of recording and high sound quality. Some have taken advantage of these advances to create libraries of heart and lung sounds, providing an effective way to teach students this medical art (Arjoune, 2023).

It is noted that the characterisation of sounds through auscultatory signal recording, analysis and processing systems provides improved sensitivity and specificity in various studies. Furthermore, the availability of new representations of sounds, such as phonograms and spectrograms, not only opens up interesting perspectives in the context of diagnostic aids, but also in education and pedagogy (Emmanuel, 2016). This will allow medical students and trainees to perform realistic cardiac auscultations and listen to abnormal heart sounds in a clinical setting (Yhdego,2023).

ISSN: 2523-2517

The conversion of acoustic sound into an electrical signal requires a transducer. There are several types of transducers that can perform this function. The simplest method of sound detection is the use of a microphone in the chestpiece of the stethoscope. However, this technique has a drawback: it is susceptible to interference from ambient noise. An alternative is to place a piezoelectric crystal on the end of a metal shaft that is in contact with a diaphragm. Some manufacturers use more sophisticated methods, such as placing a piezo crystal inside a foam behind a diaphragm of considerable thickness, similar to rubber. Another technique involves the use of an electromagnetic diaphragm with a conductive inner surface that forms a capacitive sensor. This diaphragm responds to sound waves in a similar way to a conventional acoustic stethoscope, but with the difference that changes in the electric field replace changes in air pressure. The sound waves interacting with the condenser microphone generate a variation in its capacitance. This variation creates a voltage swing that is proportional to the amplitude of the incident sound waves. Correct positioning of the acoustic sensor relative to the microphone is essential to capture sound signals from the human body without noise interference. The microphone should be positioned as close as possible to the diaphragm. An electrical cable of sufficient length is provided linking the microphone to the connection plug, thus ensuring that there is room to properly position the sensor on the patient (Khandpur, 2020).

There are applications that describe in detail the setup of a system using the AD8232 module connected to an Arduino development board to acquire electrical signals from the heart. The AD8232 module is able to amplify and filter the ECG signal to obtain an accurate measurement, where a user interface is included in the form of a mobile application, which allows users to view and analyse the ECG data in real time, this application graphically displays the ECG waveform and provides information about the heart rate and possible cardiac abnormalities. This system shows a very good correlation between the data obtained between the application and traditional equipment found in hospitals and can be a viable alternative for cardiac monitoring (Prasad, 2019).

There are relevant developments such as the one carried out in Indonesia, where approximately 700,000 deaths per year are caused by heart attacks. To prevent heart attacks from becoming serious, early diagnosis is of utmost importance. One of the diagnostic techniques is the electrocardiogram (ECG). ECG devices record the electrical signal of the heart muscle to predict the presence of abnormalities in the heart. However, most of the existing ECG devices in Indonesia are found only in large hospitals. Patients with a heart attack have to wait for the ambulance to arrive and take them to the hospital. While waiting for the ambulance, the important signal associated with the heart attack may diminish, causing doctors to lose track of the causes of the heart attack. Other patients are too busy to have an ECG check unless something goes wrong with their heart. The ECG check is annoying. Therefore, it is very important to develop portable ECG devices. The portability of the devices will allow them to be placed in a Puskemas, which is a community health centre in Indonesia that offers primary health care services, and even in people's homes. Diagnosis will also be much easier and cheaper. Special conditions, such as heart attack patients, can also be taken care of with a portable ECG home care device (Gifari, 2015).

In this work a monitoring system was developed using a graphical interface developed with Matlab software, connected to an Arduino development board implementing an AD8232 module to visualise the behaviour of the acquired data and analyse ECG data, complemented with a stethoscope replacing the headphones with electret microphones connected to a preamplifier and fourth order active filters with Sallen-Key configuration, which could be beneficial for the diagnosis and monitoring of cardiac diseases, this proposed system seeks to provide an accessible and portable solution.

Aim

The main objective of this project is to design an electronic stethoscope using second order active filters and TL081CP operational amplifiers. The stethoscope will be intended to listen to the acoustic signals generated by the heart and lungs. In addition, a graphical interface will be designed using an Arduino UNO development board to acquire data.

ISSN: 2523-2517

For this, an AD8232 module will be used to compare the acoustic signal captured by the stethoscope with the signal coming from an ECG module. The collected data will be stored in a microSD memory by using a microSD card reader module. In addition, we plan to design a printed circuit board that will serve as the basis for assembling the Arduino UNO development board. This board design will facilitate the connection between the different modules used, such as the AD8232, RTC-DS3132 and the microSD card reader. The aim of this board is to avoid the excessive use of wires, reduce noise generation and minimise parasitic capacitances.

Hypothesis

In recent years, academics and students of the Electrical and Electronic Engineering course at the Facultad de Estudios Superiores Aragón at the Universidad Nacional Autónoma de México have faced challenges in the development of projects. One of the current challenges is to find innovative and creative solutions to address health issues in a society that has been seriously affected by the pandemic. In particular, the post-pandemic phase has left cardiac sequelae in patients who had comorbidities prior to SARS-CoV2. If an electronic stethoscope is developed that implements OPAM (Operational General Purpose Amplifier) filters for the observation of cardiac signals, using a graphical interface with an AD8232 module, then a significant benefit could be gained for the diagnosis and monitoring of cardiac disease, the system provides an accessible, portable and inexpensive solution to improve the detection and monitoring of cardiac disease.

Methodology and Development

This work was carried out in the Measurement, Instrumentation and Control Laboratory of the Centro Tecnológico Aragón of the FES. Aragón UNAM. A test board (Protoboard) was used to build a microphone preamplifier as shown in Figure 1, the eletcret will be adapted to the inside of the stethoscope ear tubes, an investigation on the use of low-pass filters to isolate low-frequency sounds was carried out.

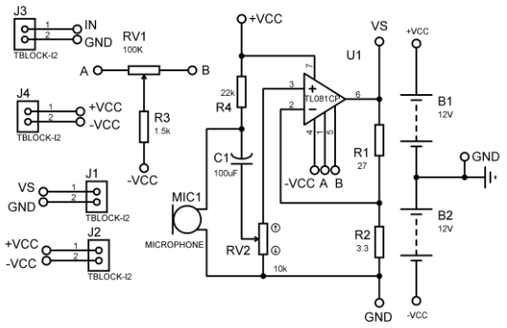

Figure 1 Circuit design for the cardiac signal preamplifier using an integrated TL081CP

Primarily, it is necessary to convert the heart sound into an electrical signal. To achieve this, a conventional stethoscope was modified by adding electro-acoustic (electret) microphones, as shown in Figure 1. In this way, the captured sound can be transformed into an electrical signal, which can then be processed by low-pass filters.

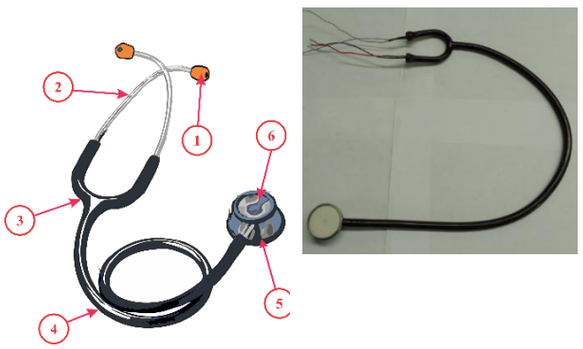

(a) (b)

Figure 2 a) Structure of the stethoscope. 1. Eyepieces 2. Earpieces 3. Bell. b) Modified stethoscope with two electret stethoscopes with preamplifier connection cables as shown in Figure 1.

The stethoscope, a fundamental instrument in medical practice, is used to amplify the internal sounds of the human body, facilitating auscultation. This device consists of several elements. Firstly, the end piece, which is placed on the patient's skin, has two parts: a semi-rigid membrane that is used to detect sounds of normal intensity, and a cup designed to capture softer sounds. When sound waves hit the membrane or bell, they begin to vibrate and amplify the sounds. The sound waves are then transmitted through a Y-shaped hose, made of a soft, flexible material, with a standard length of 40 cm.

ISSN: 2523-2517

The two ends of the "Y" are attached to two metal terminals (earpieces), each intended for one ear. These earpieces culminate in two ear-tips that fit snugly into the ear canal, capturing all transmitted sound and isolating outside noise that might interfere. In this way, the stethoscope allows the healthcare professional to clearly hear the internal sounds of the patient's body (Mesa, 2021). Recently, digital stethoscopes are replacing traditional stethoscopes due to their technological advantages in accuracy and data analysis. Auscultation, a widely used medical technique, becomes relevant with these advances, providing important details about cardiovascular and pulmonary diseases. Only medical experts in respiratory sounds, such as pulmonologists or cardiologists, can properly interpret these sounds and provide accurate diagnoses (Chitra, 2023).

Figure 3 shows a second-order low-pass filter circuit assembled on a test board. Although this system allows the heart sound to be heard through a loudspeaker, the intensity of the sound is low due to the attenuation of the acoustic signal as it passes through the filter. It should be noted that body noises are in the frequency range of 125 Hz to 3000 Hz, according to Lanuza (2019). However, due to the aforementioned attenuation, these sounds may not be easily perceptible.

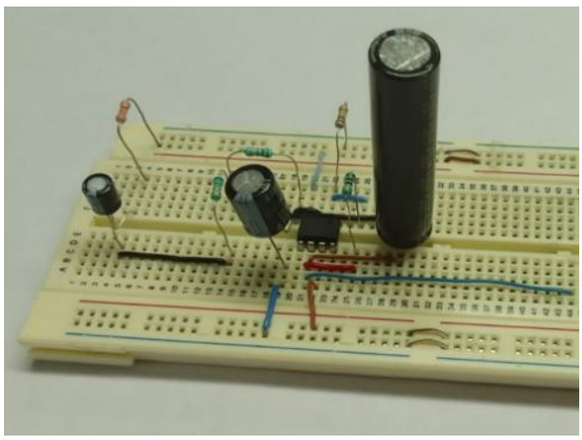

Figure 3 Breadboard circuit design of the preamplifier with a 10 gain op amp

The audio signal, once transformed into an electrical signal, is amplified by a preamplifier. Human heart sounds oscillate in a frequency range of about 20-200 Hz, while human lung sounds oscillate in a range of about 25-1500 Hz.

Most commercially available electronic stethoscopes offer several modes, including bell mode, diaphragm mode and extended range mode. These stethoscopes are equipped with a button or switch to change the frequency or mode, which may be located on the chestpiece, on a module integrated in the tube, or even directly on the main unit of the stethoscope. A set of filters is responsible for amplifying mid-range sounds, while attenuating sounds with extremely high or low frequencies. The extended range, on the other hand, is often referred to as wide, extended or organ mode.

A filter is a circuit or system designed to select, attenuate or eliminate certain frequency ranges within an input signal. It has both an input and an output. At the input, alternating signals with various frequencies are input, while at the output, these signals are extracted. Depending on the frequency of the signal, these can be attenuated to a greater or lesser extent. This filter, known as a low-pass filter, allows all frequencies from zero to a certain cut-off frequency to pass through, blocking all frequencies above this frequency. The frequencies between zero and the cutoff frequency are called the passband. On the other hand, frequencies above the cut-off frequency are called the passband or the attenuated band. The area between the passband and the removed band is known as the transition region (Mendoza, 2018).

Therefore, we have concluded that it is best to use a frequency of 690 Hz. This would allow us to effectively isolate the sound produced by the heart and lungs, allowing us to hear the acoustic waves more clearly. To achieve this goal, we sought to configure a second-order non-inverting Sallen-Key active low-pass filter.

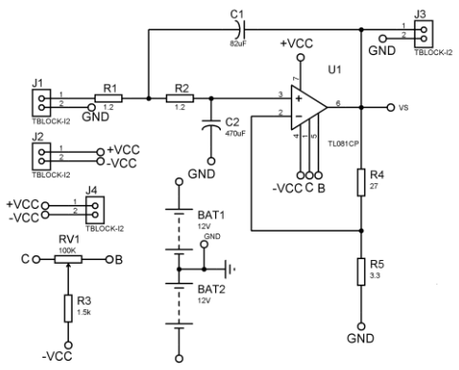

Figure 4 Schematic circuit design of a second-order Sallen-Key low-pass filter with a TL081CP housing

ISSN: 2523-2517

Figure 4 shows terminals B and C. Here, it can be seen that Pin 1 of the OPAM is connected to the first terminal of the component known as the trimmer (C), while Pin 5, according to the circuit diagram label, is connected to the third terminal of the trimmer (B).

In the data sheet for the ideal operational amplifier, the inverting input is denoted as V- or V_n, and is connected to terminal 2 of the package. On the other hand, the non-inverting input, which can be represented as V+ or V_p, is connected directly to terminal 3 of the TL081CP. This results in the voltages V_n and V_p at both terminals being equal, as shown in Equation 1 for an ideal operational amplifier. This condition is known as 'virtual balance', and is an important property of operational amplifiers, widely used in various circuits that require signal amplification or in filters that discriminate signals of certain frequencies. In certain experimental set-ups, small differences in input terminal voltages have been observed, attributable to component imperfections and external noise interference. However, for practical purposes, it was assumed that the voltages can be expressed as indicated in Figure 2 shows the B and C terminals. Here, it can be seen that Pin 1 of the OPAM is connected to the first terminal of the component known as the trimmer (C), while Pin 5, according to the circuit diagram label, is connected to the third terminal of the trimmer (B).

In the data sheet for the ideal operational amplifier, the inverting input is denoted as V- or V_n, and is connected to terminal 2 of the package. On the other hand, the non-inverting input, which can be represented as V+ or V_p, is connected directly to terminal 3 of the TL081CP. This results in the voltages V_n and V_p at both terminals being equal, as shown in Equation 1 for an ideal operational amplifier. This condition is known as 'virtual balance', and is an important property of operational amplifiers, widely used in various circuits that require signal amplification or in filters that discriminate signals of certain frequencies. In certain experimental set-ups, small differences in input terminal voltages have been observed, attributable to component imperfections and external noise interference. However, for practical purposes, it was assumed that the voltages can be expressed as follows.

$$V_n=V_p \tag{1}$$

In Figure 2 it can be seen that the input of pin 2 is connected to V_n with two connected resistors R_4 which would represent the feedback resistor R_f connected at the other end to V_s which indicates the output voltage of the filter represented with Pin 6 and R_5 is represented as R_i which together can be obtained as a voltage divider as shown in Equation 2.

$$V_n=\frac{R_i V_s}{R_i+R_f} \tag{2}$$

By subtracting the output voltage *Vs* from Equation 2.

$$V_s=\left(1+\frac{R_f}{R_i}\right)V_n \tag{3}$$

From Equation 3 we can substitute the part inside the parentheses and represent it as the closed-loop gain by Δv .

$$V_n=\frac{V_s}{\Delta v} \tag{4}$$

The equilibrium equations are established, starting at node V_x by applying Kirchhoff summation currents as shown in Equation 5.

$$\frac{V_p}{R_2}-\frac{V_x}{R_2}+V_p sC_2=0 \tag{5}$$

The second equilibrium equation is established at node V_x by applying Kirchhoff summation currents as shown in Equation 6,

$$\frac{V_x-V_i}{R_1}+\frac{V_x-V_p}{R_2}+\frac{V_x-V_s}{\frac{1}{sC_1}}=0 \tag{6}$$

From Equation 5 we obtain V_x

$$V_p(1+sR_2C_2)=V_x \tag{7}$$

From Equation 7 we apply the equality of Equation 1 and substitute Equation 4 to obtain the following equation as a function of V_s, where we will later have the ratio of the output voltage to the input voltage to visualise the transfer function of the second order low-pass filter.

$$\frac{V_s}{\Delta v}(1+sR_2C_2)=V_x \tag{8}$$

ISSN: 2523-2517

Starting from Equation 6 and developing the corresponding algebra, V_x is cleared and the following equation is obtained.

$$V_x=\frac{V_iR_2+V_pR_1+V_ssR_1R_2C_1}{R_2+R_1+sR_1R_2C_1} \quad (9)$$

From Equation 8 and Equation 9 both equations equal each other since they have the common term V_x, as follows.

$$\frac{V_s}{\Delta v}[1+sR_2C_2]=\frac{V_iR_2+\frac{V_s}{\Delta v}R_1+V_ssR_1R_2C_1}{R_2+R_1+sR_1R_2C_1} \quad (10)$$

Both sides of the equality we have the output voltage V_s, which is a common term and we have the input voltage V_i. Obtaining the ratio of the input voltage with respect to the output we have the following equation;

$$\frac{V_s}{V_i}=\frac{\Delta v}{s^2R_1R_2C_1C_2+s(R_1C_1+R_2C_2+R_1C_2-R_1C_1\Delta v)+1}$$

Simplifying the above equation:

$$\frac{V_s}{V_i}=\frac{\Delta v}{s^2R_1R_2C_1C_2+s\big(C_2(R_1+R_2)+R_1C_1(1-\Delta v)\big)+1} \quad (11)$$

This results in the transfer function as shown in Equation 12, where it can be seen in both the numerator and the denominator that the gain is involved in the polynomial.

$$H(s)=\left(\frac{\Delta v}{R_1R_2C_1C_2}\right)\left(\frac{1}{s^2+s\left(\frac{C_2(R_1+R_2)+R_1C_1(1-\Delta v)}{R_1R_2C_1C_2}\right)+\frac{1}{R_1R_2C_1C_2}}\right) \quad (12)$$

The angular cutoff frequency is given by ω_c

$$\omega_c^2=\frac{1}{R_1R_2C_1C_2}\rightarrow\omega_c=\sqrt{\frac{1}{R_1R_2C_1C_2}}\rightarrow\omega_c=\frac{1}{\sqrt{R_1R_2C_1C_2}} \quad (13)$$

The quality factor is given by

$$\frac{\omega_c}{Q}=\frac{C_2(R_1+R_2)+R_1C_1(1-\Delta v)}{R_1R_2C_1C_2}$$
$$Q=\frac{\omega_c(R_1R_2C_1C_2)}{C_2(R_1+R_2)+R_1C_1(1-\Delta v)}$$
$$Q=\frac{\frac{(R_1R_2C_1C_2)}{\sqrt{R_1R_2C_1C_2}}}{C_2(R_1+R_2)+R_1C_1(1-\Delta v)} \quad 14)$$

It can be seen that in Figure 2 the resistance R_1 and R_2 are equal $R_1=R_2=R$

$$H(s)=\left(\frac{\Delta v}{R^2C_1C_2}\right)\left(\frac{1}{s^2+s\left(\frac{(2C_2+C_1(1-\Delta v))}{RC_1C_2}\right)+\frac{1}{R^2C_1C_2}}\right) \quad (15)$$

Calculating the angular cutoff frequency which has as its units of $\left[\frac{rad}{s}\right]$

$$\omega_c=\frac{1}{R\sqrt{C_1C_2}} \quad (16)$$

If we condition that the values of the passive elements in this case the resistor $R_1=R_2$ and the capacitor $C_1=C_2$ are equal we have the following expression.

$$H(s)=\frac{\Delta v}{s^2R^2C^2+sRC(3-\Delta v)+1} \quad (17)$$

From the equation we normalise to identify the cut-off frequency as shown in the equation below:

$$H(s)=\left(\frac{\Delta v}{R^2C^2}\right)\left(\frac{1}{s^2+s\left(\frac{3-\Delta v}{RC}\right)+\frac{1}{R^2C^2}}\right) \quad (18)$$

Another way to represent the normalised transfer function is to replace the gain Δv with the variables of the resistors involved as follows R_f and R_i

$$H(s)=\left(\frac{1+\frac{R_f}{R_i}}{R^2C^2}\right)\left(\frac{1}{s^2+s\left(\frac{3-\left(1+\frac{R_f}{R_i}\right)}{RC}\right)+\frac{1}{R^2C^2}}\right) \quad (19)$$

Substituting the values of the resistances for the conductance gives the transfer function, which would be represented as shown in the following equation:

$$H(s)=\frac{\Delta vG_1G_2}{s^2C_1C_2+s(C_2(G_1+G_2)+C_1G_2(1-\Delta v))+G_1G_2} \quad (20)$$

By substituting the inverses of the resistors, when the balance equations are established at the time of the Kirchhoff current summation analysis, Equation 10 of the same transfer function can be arrived at. Gain as a function of voltage or power can be used.

$$dB=20\log_{10}(\Delta v)=20\log_{10}(1+\frac{R_f}{R_i}) \quad (21)$$

It should be noted that the dB voltage gain is only equal to the dB power gain if the input and output impedances of the system match.

ISSN: 2523-2517

$$dB_{rms}=20\log_{10}\left(\frac{\Delta v}{\sqrt{2}}\right)=20\log_{10}\left(\frac{1+\frac{R_f}{R_i}}{\sqrt{2}}\right) \quad (22)$$

To obtain the quality factor, it can be obtained as shown in the following equation.

$$Q=\frac{\sqrt{C_1C_2}}{\left(2C_2+C_1(1-\Delta v)\right)} \quad (23)$$

To make the Bode plot in magnitude and phase, the simplified Equation 12 was taken, taking the following values for its design, where: $R=R_1=R_2=1.2\Omega$, $C_1=82uF$, $C_2=470uF$, $R_f=27\Omega$ and $R_i=3.3\Omega$ the frequency used is f =675 Hz the calculation of the angular frequency is $\omega_c=4244.9\left[\frac{rad}{s}\right]$ this comes from Equation 13, to calculate the Gain $\Delta v=1+\frac{R_f}{R_i}=9.1818$ the unit of this is dimensionless, if we take this value we can obtain the decibels applying Equation 18 giving as a result dB=19.2586 and to obtain the decibels of the root mean square is obtained from Equation 19 and gives as a result $dB_{rms}=16.2483$ which is exactly where it cuts the angular cutoff frequency, its quality factor Q= 0.7296 is also obtained through Equation 20. Therefore, substituting the values of the passive elements in the transfer function would be as shown in Equation 19.

$$H(s)=\left(\frac{9.182}{5.55\times10^{-8}\,s^2+0.0003229\,s+1}\right) \quad (24)$$

Graph 2, which is derived from Equation 19, represents the Bode plot in phase and magnitude. It can be seen that its behaviour is consistent with a second-order low-pass filter, since a decade later it drops by 40dB. In the magnitude diagram, the blue arrow indicates exactly where the angular frequency intersects the root-mean-square decibels (〖dB〗 _rms). In the phase diagram, also indicated by a blue arrow, it can be seen that the cut-off angular frequency intersects at 90°.

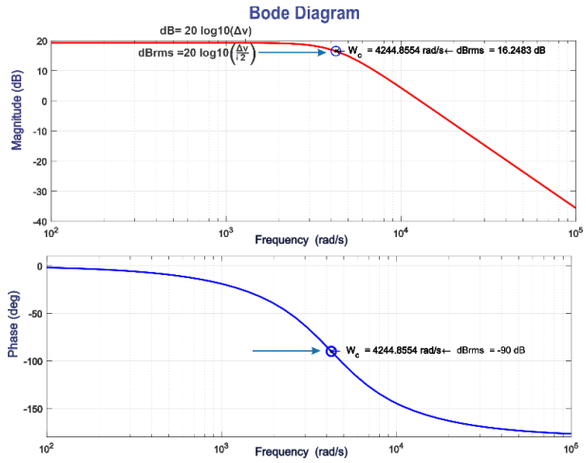

Graphic 2 Bode plot in magnitude and phase showing the cutoff angular frequency

In Graph 3, it shows the bode diagram in magnitude and phase, using the simulation program called proteus, the proposed schematic circuit was designed to implement it in the electronic stethoscope in order to filter the noise signals, noting that both graphs coincide showing the same value of ω_c and dB_{rms}.

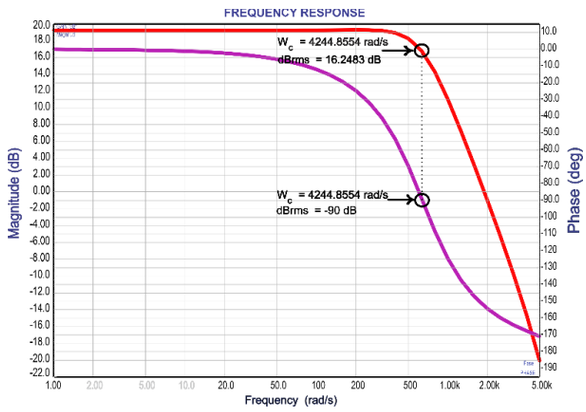

Graphic 3 Simulation using proteus of the Bode plot in magnitude and phase

For the volume control in the speaker connected to the stethoscope, a preamplifier was designed, which uses a TL081CP operational amplifier as shown in the 3D design of figure 5.

ISSN: 2523-2517

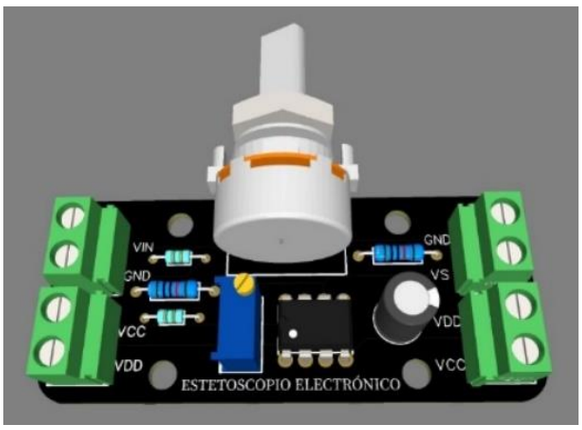

Figure 5 3D printed circuit of the preamplifier with a TL081CP package.

Figure 6 presents the three-dimensional layout of the printed circuit for the Sallen-Key second-order active low-pass filter. This circuit is composed of passive elements that will be connected to the preamplifier. In turn, these elements will receive power from the power supply of the same preamplifier. At the output of the circuit, a connection to the loudspeaker will be made.

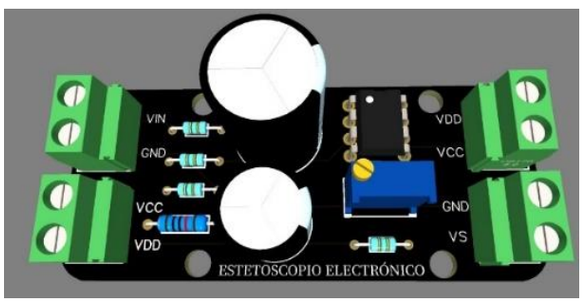

Figure 6 Three-dimensional printed circuit board of a non-inverting active second-order low-pass filter

Figure 7 shows the layout of the printed circuit in which the passive components, such as the resistor and the capacitor, will be mounted. The terminal blocks will also be installed, which will allow energy to be transferred from one plate to another, and transmit the acoustic signal from the stethoscope so that it can be heard through the loudspeaker.

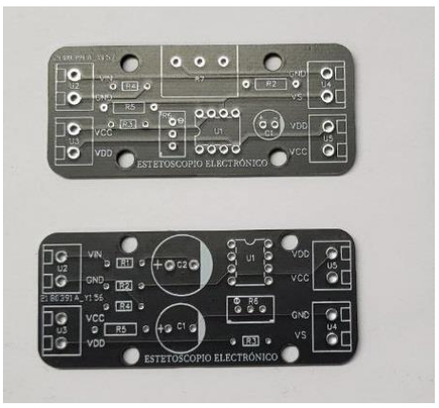

Figure 7 Active 2nd Order Low Pass Filter and Preamplifier PCB

It is crucial to properly layout the printed circuit board with the corresponding traces, which will allow the manufacturer to silk-screen print the precise dimensions. This layout is essential during component assembly, as it facilitates the identification of polarisation indications and the correct placement of integrated circuits. By following these guidelines, the generation of short circuits can be prevented, as illustrated in Figure 8.

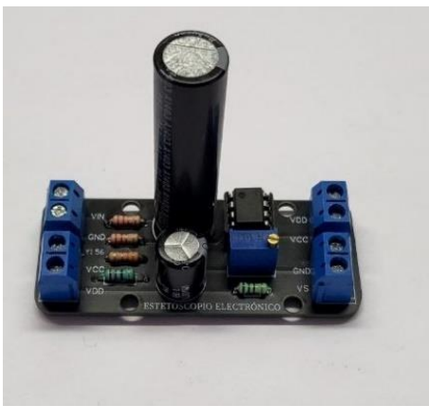

Figure 8 Electronic circuit board with the passive elements of the second order active low-pass filter to be assembled to the preamplifier and the speaker

For the design of the graphical interface of the electronic stethoscope, a printed circuit board was developed that allows the integration of the Arduino UNO development board with various modules. These modules include the AD8232, the RTC-DS3132 and a MicroSD Reader. These components are assembled and connected according to the schematic circuit shown in Figure 3.

ISSN: 2523-2517

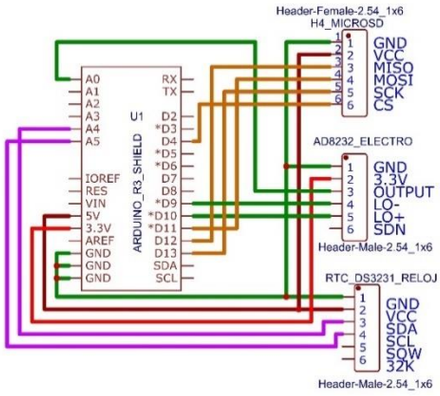

Figure 9 Design of the shelft schematic circuit to attach it to the Arduino development board and mount the modules RTC-DS3231, AD8232 and the MicroSD module

Figure 7 presents the design of a three-dimensional printed circuit board, developed using online computer-aided design software. This design clearly details the silk-screen printing of the modules to be used for the experiment.

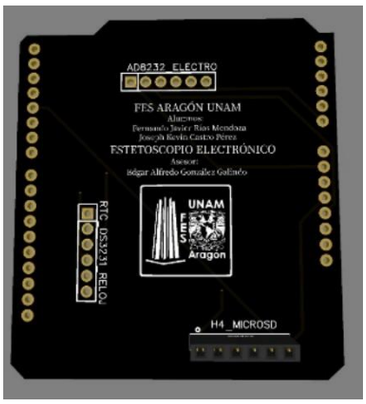

Figure 10 3D printed circuit board for connection between Arduino uno and AD8232 modules, RTC-DS3132, microSD card reader

The physical design of a printed circuit board (PCB) is of great importance due to the many advantages it offers during operation. One of the main advantages is the elimination of much of the noise that is often generated by the connection cables, which can act as electrical dipoles. The purpose of this design is to facilitate the assembly and disassembly of each module. For this reason, female connectors have been incorporated into the design to allow easy replacement by the operator in the event of damage. This can be seen in Figure 8.

Figure 11 Printed circuit board for connection of AD8232, RTC-DS3132, microSD card reader modules

Image 8 below shows the development board used in the experimental setup, as well as the printed circuit board that will be placed on top of the Arduino UNO.

Figure 12 Printed circuit board for the connection between the Arduino uno and the modules AD8232, RTC-DS3132, microSD card reader

The modules used that will be mounted on the PCB layout are shown in Figure 10, together with the development board and the PCB circuit.

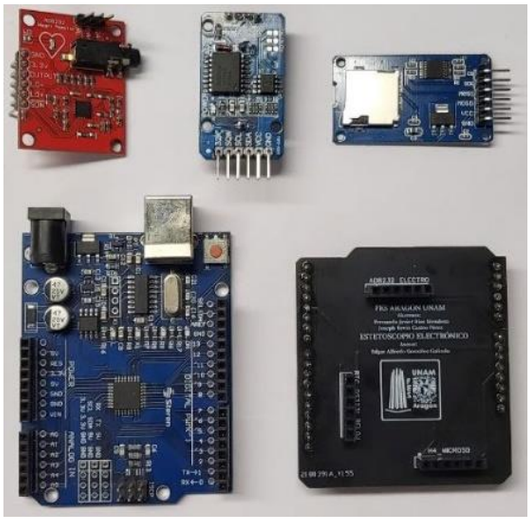

Figure 13 AD8232, RTC-DS3132 and microSD card reader modules, together with development board and PCB

ISSN: 2523-2517

Figure 11 shows the assembly of the AD8232, RTC-DS3132 and microSD card reader modules on the PCB mounted on the Arduino UNO.

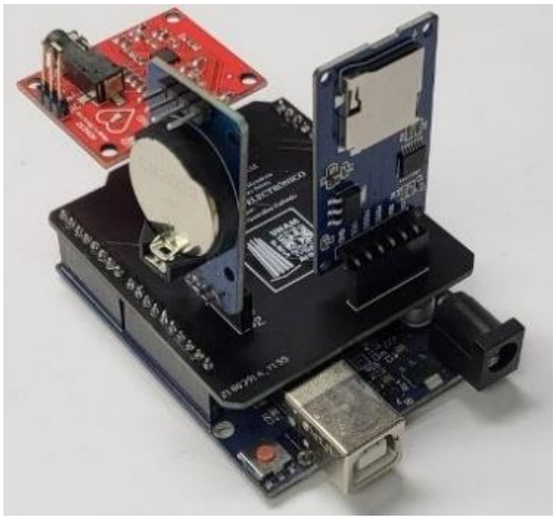

Figure 14 Printed circuit board with the assembled modules on the Arduino UNO development board

The following code is used to obtain data from the ECG module. This code collects information such as date, time and data logging for the electrical signal. The collected sampling is used to plot the electrical signal using the serial plotter in the Arduino integrated development environment (IDE).

```
//Se incluyen las siguientes librerías para poder programar los módulos
#include <Wire.h>
#include <RTClib.h>
#include <SD.h>
#include <SPI.h>
//Inicializar el objeto para manejar la lectura del RTC-DS3132
RTC_DS3231 rtc;
//Variable para guardar el tiempo actual del RTC
DateTime now;
//Variable para guardar la lectura del AD8232
int ecgValue;
//Variable para el nombre del archivo en la tarjeta microSD
char filename[] = "dataecg.txt";
//Variable para el pin CS del módulo lector de microSD
const int chipSelect = 4;
void setup() {
  //Inicializar el puerto serie
  Serial.begin(9600);
    //Inicializar la comunicación con el RTC
  Wire.begin();
  rtc.begin();
    //Inicializar la comunicación con la tarjeta microSD
  if (!SD.begin(chipSelect)) {
    Serial.println("Error al inicializar la tarjeta microSD.");
    return;
  }
    //Crear el archivo para guardar las lecturas
  File dataFile = SD.open(filename, FILE_WRITE);
    //Verificar si se pudo crear el archivo
  if (dataFile) {
    dataFile.println("Fecha, Tiempo, ampm, Valor ECG");
    dataFile.close();
    Serial.println("Archivo creado.");
  } else {
    Serial.println("Error al crear el archivo.");
  }
}
void loop() {
  //Leer el tiempo actual del RTC
  now = rtc.now();
    //Leer el valor del AD8232
  ecgValue = analogRead(A0);
    //Abrir el archivo para agregar una nueva lectura
  File dataFile = SD.open(filename, FILE_WRITE);
    //Verificar si se pudo abrir el archivo
  if (dataFile) {
    //Agregar la lectura al archivo
    dataFile.print(now.year(), DEC);
    dataFile.print('/');
    dataFile.print(now.month(), DEC);
    dataFile.print('/');
    dataFile.print(now.day(), DEC);
    dataFile.print(',');
    dataFile.print(' ');
    dataFile.print(now.hour(), DEC);
    dataFile.print(':');
    dataFile.print(now.minute(), DEC);
    dataFile.print(':');
    dataFile.print(now.second(), DEC);
    dataFile.print(',');
    dataFile.println(ecgValue);
    dataFile.close();
    //Imprimir la lectura en el puerto serie
    Serial.print(now.year(), DEC);
    Serial.print('/');
    Serial.print(now.month(), DEC);
    Serial.print('/');
    Serial.print(now.day(), DEC);
    Serial.print(',');
    Serial.print(' ');
    Serial.print(now.hour(), DEC);
    Serial.print(':');
    Serial.print(now.minute(), DEC);
    Serial.print(':');
    Serial.print(now.second(), DEC);
    Serial.print(',');
    Serial.println(ecgValue);
  } else {
    Serial.println("Error al abrir el archivo.");
  }
    //Esperar un segundo antes de tomar otra lectura
  delay(1000);
}
```

Results

Figure 11 shows the configuration of eight modules each comprising the preamplifiers and the second order active low-pass filters. These modules are combined to form a fourth order filter.

ISSN: 2523-2517

The output signals from these modules are connected to an audio amplifier, which in turn is connected to the loudspeakers. Both the loudspeakers and the complete system are powered by a voltage source for proper biasing. To carry out the tests, a high-performance subject was selected. Over a period of 30 minutes, acoustic sounds corresponding to the subject's heart rate were recorded and obtained.

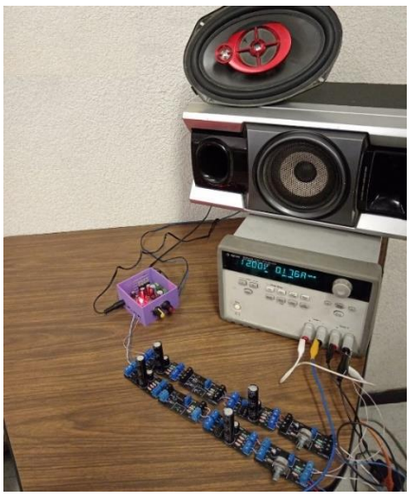

Figure 15 Experimental arrangement integrated by modules of the filters using and of the audio amplifier

During the test to obtain the acoustic signal of the heart rate, the subject was asked to maintain a proper position, as shown in Figure 12, and was instructed to remove the T-shirt to allow for proper auscultation. The subject was instructed to maintain normal breathing and muscle relaxation to facilitate an accurate assessment. As a result, a clear heart rate signal was obtained, ruling out other acoustic signals coming from the same subject, such as abdominal sounds, vascular sounds and joint sounds. This allowed a better focus on the auscultation of the heart rhythm and contributed to a more accurate assessment.

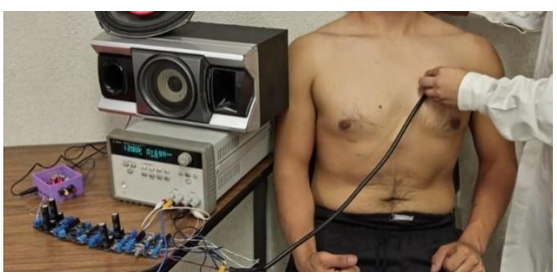

Figure 15 Test carried out on a subject, after physical activity, using a Sallen-Key fourth-order active low-pass filter

The results of connecting the modules to observe the synchronisation between the acoustic signal and the behaviour of the electrical signal coming from the AD8232 module are presented below, as illustrated in Figure 13. During the tests, it was possible to simultaneously obtain a visual representation of the electrical signal and the perception of an acoustic signal corresponding to the heart rhythm. This approach allowed the visualisation and auditing of the electrical and acoustic activity of the heart together, providing a comprehensive and complementary assessment of the heart rhythm during the test period.

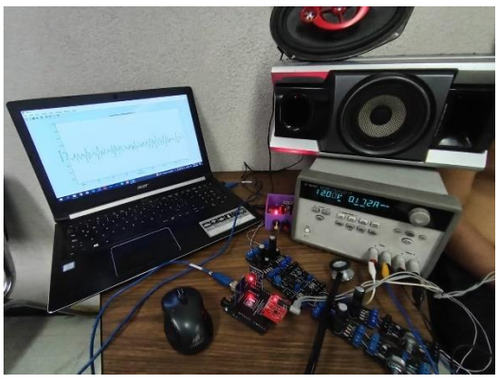

Figure 16 Experimental fix implementing the modules AD8232, RTC-DS3132, microSD card reader. Visualizing in a graphical interface the electrical signal coming from the heart rate.

A visual representation of the data recorded by the AD8232 module was obtained in Graph 4, where the amplitude variations that are characteristic of a cardiac signal can be clearly observed.

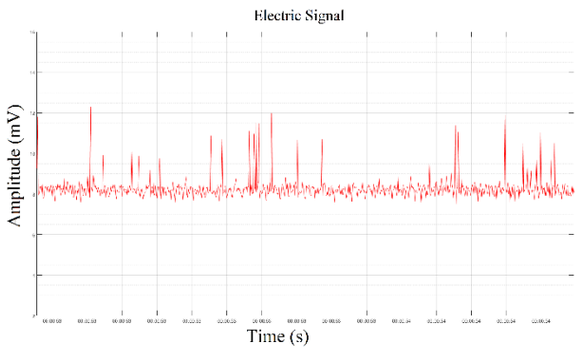

Graphic 4 Record of the electrical signal displayed in real time through the graphical interface from the AD8232 module

ISSN: 2523-2517

The initial electrical signal, captured by the AD8232, was subjected to processing using a digital band-pass filter. This filter was designed to eliminate certain signals with specific frequencies, which allowed a smoother signal to be obtained, free of unwanted interference. The results of this processing are presented in Figure 5.

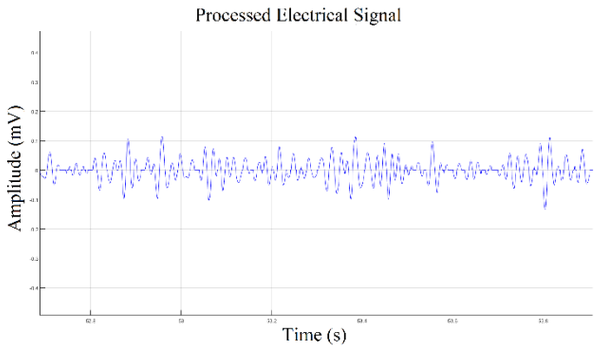

Graphic 5 Electrical signal passed through the digital fifth order band-pass filter

Conclusion

An electronic stethoscope has been designed and developed using second order active filters with TL081CP operational amplifiers. This will allow the acoustic signals generated by the heart and lungs to be heard clearly and accurately in a loudspeaker and by using a graphic interface implemented on an Arduino UNO development board, it has been possible to acquire and visualise the data collected by the ECG module. This interface will provide students of Electrical and Electronic Engineering and Medicine with a practical and user-friendly tool for monitoring cardiac and respiratory signals. The integration of the AD8232 module has made it possible to compare the acoustic signal captured by the stethoscope with the signal coming from an ECG module. This comparison provides greater accuracy in the diagnosis and analysis of cardiac signals. Data collected during measurements are conveniently stored on a microSD memory, using an SD card reader module. This ensures data availability and portability for further analysis and review. The design of a printed circuit board specifically for this project has enabled an efficient connection between the different modules used, reducing noise generation and minimising parasitic capacitances compared to using a test board called Protoboard.

This improves the quality of the acquired electrical signals and provides a stable platform for the operation of the electronic stethoscope. In summary, the stated objectives have been met by developing a functional electronic stethoscope with cardiac and respiratory signal acquisition and display capabilities. This device presents advantages in terms of cost, accuracy, portability and ease of use, which contributes to improving medical care in diverse clinical situations. The work presented in this article will allow, in the future, the characterisation of electrical signals used in robotic prostheses.

Acknowledgements.

The authors would like to thank the Coordination of the Technological Centre of the Facultad de Estudios Superiores Aragón and the Electrical and Electronic Engineering Department of the Universidad Nacional Autónoma de México, for the facilities provided through agreements with different software companies. We would also like to thank Jorge Ríos Mendoza for his technical support to this project.

References

Organización Mundial de la Salud. (2023). Enfermedades cardiovasculares. Recuperado de https://www.who.int/es/news-room/fact-sheets/detail/cardiovascular-diseases-(cvds)

Bibiano Mejía, I., & González Galindo, E. A. (2023). Diseño e implementación de una tarjeta de circuito impreso para acoplar módulos y generar un instrumento electrónico de medición de pulso y oxígeno para detección de cardiopatías y control de medicamentos en pacientes diagnosticados. http://132.248.9.195/ptd2023/abril/0838030/Index.html

Roguin, A. (2006). Rene Theophile Hyacinthe Laënnec (1781–1826): The Man Behind the Stethoscope. Clinical Medicine & Research, 4(3), 230–235. https://doi.org/10.3121/cmr.4.3.230

Langfort J, Ploug T, Ihlemann J, Saldo M, Holm C, Galbo H. Expression of hormone-sensitive lipase and its regulation by adrenaline in skeletal muscle. Biochem J. 1999 Jun 1;340 (Pt 2)(Pt 2):459-65. PMID: 10333490; PMCID: PMC1220272.

ISSN: 2523-2517

Emmanuel Andrès, Raymond Gass (2016), Stethoscope: A Still-Relevant, Tool and Medical Companion, The American Journal of Medicine,Volume 129, Issue 5, 2016, Pages e37-e38. https://doi.org/10.1016/j.amjmed.2015.06.046.

Yhdego, H., Kidane, N., Mckenzie, F. y Audette, M. (2023). Desarrollo de modelos de aprendizaje profundo para una simulación híbrida de entrenamiento de auscultación en pacientes estándar utilizando un estetoscopio de patología virtual basado en ECG. SIMULACIÓN , 00375497231165049. https://doi.org/10.1177/00375497231165049

A. S. Prasad and N. Kavanashree, "ECG Monitoring System Using AD8232 Sensor," 2019 International Conference on Communication and Electronics Systems (ICCES), Coimbatore, India, 2019, pp. 976-980, https://doi:10.1109/ICCES45898.2019.9002540.

M. W. Gifari, H. Zakaria and R. Mengko, "Design of ECG Homecare:12-lead ECG acquisition using single channel ECG device developed on AD8232 analog front end," 2015 International Conference on Electrical Engineering and Informatics (ICEEI), Denpasar, Indonesia, 2015, pp. 371-376, https://doi:10.1109/ICEEI.2015.7352529.

Mesa, A. L. U., & Moreno, D. U. (2021). Manual para el examen físico del normal y métodos de exploración. Corporación para investigaciones Biológicas CIB. URL: https://books.google.com.mx/books?id=mtQwEAAAQBAJ&pg=SA4-PA25&dq=estetoscopio+electr%C3%B3nico&hl=es-419&sa=X&ved=2ahUKEwiywsD1vsL8AhVgEUQIHXsmA04Q6AF6BAgJEAI#v=onepage&q=estetoscopio%20electr%C3%B3nico&f=false

R. Chitra, N. Jayapreetha, D. Swetha y S. Swetha, "Digital Stethoscope For Instant Monitoring For Cardiac Auscultation", Conferencia internacional de 2023 sobre señales biológicas, imágenes e instrumentación (ICBSII) , Chennai, India, 2023, págs. 1-6, https://doi:10.1109/ICBSII58188.2023.10181065

Lanuza Centeno, J. E., & Moncada Flores, C. A. (2019). Variación de los niveles de presión arterial en los pacientes sometidos a procedimientos de exodoncia en las clínicas de cirugía oral y diagnóstico de la Facultad de Odontología de la UNAN -León, en el período de agosto a noviembre del año 2017 y octubre a diciembre del año 2018, URL: http://riul.unanleon.edu.ni:8080/jspui/bitstream/123456789/7687/1/244159.pdf

Khandpur, R. S. (2020). *Compendium of biomedical instrumentation*. John Wiley & Sons, Incorporated. URL:https://www.proquest.com/docview/2319746494?accountid=14598&parentSessionId=nGD4xNVuUP3RGwMU1T4%2BcQSSOCs26ePQc9z4iL%2B4f0E%3D

Mendoza Corona, J. A., & Pérez López, M. A., (2018), Filtro pasa bajas con capacitores conmutados. URL: https://tesis.ipn.mx/bitstream/handle/123456789/27828/TESIS-FINAL.pdf?sequence=1&isAllowed=y

ISSN: 2523-2517